BRAIN COMMUNICATIONS

Distinctive alteration of presynaptic proteins in the outer molecular layer of the dentate gyrus in Alzheimer's disease

Hazal Haytural,[1,*] Tomàs Jordà-Siquier,[2,*] Bengt Winblad,[1,3] Christophe Mulle,[2] Lars O. Tjernberg,[1] Ann-Charlotte Granholm,[1,4] Susanne Frykman[1,†] and Gaël Barthet[2,†]

† These authors contributed equally to this work.
* The first two co-authors.

Synaptic degeneration has been reported as one of the best pathological correlates of cognitive deficits in Alzheimer's disease. However, the location of these synaptic alterations within hippocampal sub-regions, the vulnerability of the presynaptic versus postsynaptic compartments, and the biological mechanisms for these impairments remain unknown. Here, we performed immunofluorescence labelling of different synaptic proteins in fixed and paraffin-embedded human hippocampal sections and report reduced levels of several presynaptic proteins of the neurotransmitter release machinery (complexin-1, syntaxin-1A, synaptotagmin-1 and synaptogyrin-1) in Alzheimer's disease cases. The deficit was restricted to the outer molecular layer of the dentate gyrus, whereas other hippocampal sub-fields were preserved. Interestingly, standard markers of postsynaptic densities (SH3 and multiple ankyrin repeat domains protein 2) and dendrites (microtubule-associated protein 2) were unaltered, as well as the relative number of granule cells in the dentate gyrus, indicating that the deficit is preferentially presynaptic. Notably, staining for the axonal components, myelin basic protein, SMI-312 and Tau, was unaffected, suggesting that the local presynaptic impairment does not result from axonal loss or alterations of structural proteins of axons. There was no correlation between the reduction in presynaptic proteins in the outer molecular layer and the extent of the amyloid load or of the dystrophic neurites expressing phosphorylated forms of Tau. Altogether, this study highlights the distinctive vulnerability of the outer molecular layer of the dentate gyrus and supports the notion of presynaptic failure in Alzheimer's disease.

1 Division of Neurogeriatrics, Department of Neurobiology, Care Sciences and Society, Center for Alzheimer Research, Karolinska Institutet, 171 64 Solna, Sweden
2 Univ. Bordeaux, CNRS, Interdisciplinary Institute for Neuroscience, IINS, UMR 5297, F-33000 Bordeaux, France
3 Karolinska University Hospital, Theme Aging, 141 86 Huddinge, Sweden
4 Knoebel Institute for Healthy Aging, University of Denver, Denver 80208, CO, USA

Correspondence to: Gaël Barthet,
Univ. Bordeaux, CNRS,
Interdisciplinary Institute for Neuroscience,
IINS, UMR 5297, F-33000 Bordeaux,
France. E-mail: gael.barthet@u-bordeaux.fr

Keywords: Alzheimer's disease; postmortem human brain; hippocampus; outer molecular layer of dentate gyrus; presynaptic impairment

Received December 23, 2020. Revised February 15, 2021. Accepted March 5, 2021

Abbreviations: AD = Alzheimer's disease; CA = cornu ammonis; CPLX1 = complexin-1; EC = entorhinal cortex; IML = inner molecular layer; IR = immunoreactivity; LM = stratum lacunosum-moleculare; LUC = stratum lucidum; MAP2 = microtubule-associated protein 2; OML = outer molecular layer; RAD = stratum radiatum; STX1A = syntaxin-1A; SYNGR1 = synaptogyrin-1; SYT1 = synaptotagmin-1; VAMP2 = vesicle-associated membrane protein 2

Graphical Abstract

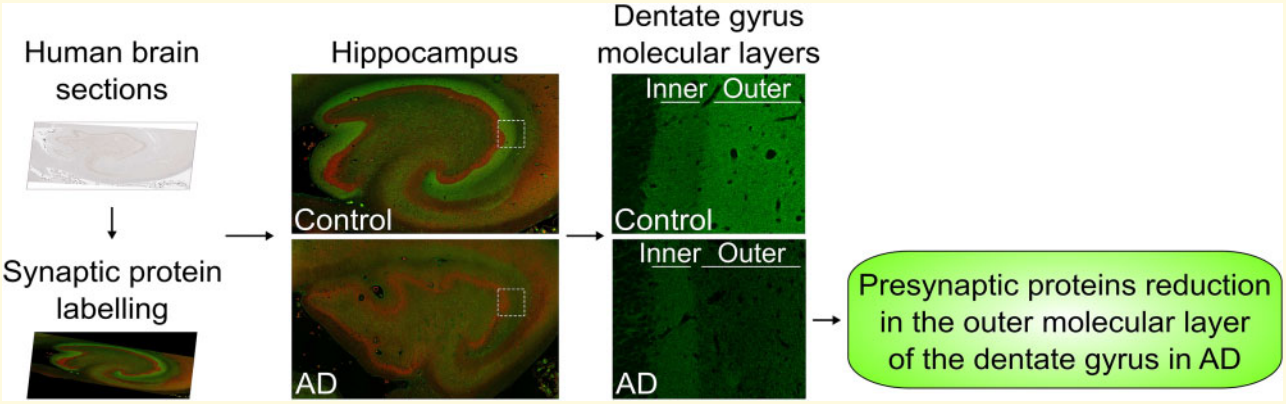

Introduction

Synaptic dysfunction and degeneration are early features in Alzheimer's disease (AD) pathogenesis and correlate well with measures of cognitive decline.[1–3] The hippocampus, a brain region which is essential for episodic memory formation is severely impaired in AD. The hippocampus consists of different anatomical regions including the dentate gyrus, the cornu ammonis (CA) regions and the subiculum[4] (Fig. 1A). The main input to the hippocampus comes from the entorhinal cortex (EC) through the perforant path[5] (Fig. 1A and C). The neurons from the layer II of the EC project to the outer two-thirds of the molecular layer of the dentate gyrus [hereafter referred as to outer molecular layer (OML); Fig. 1C] as well as to CA3, whereas the neurons from layer III project to CA1 and subiculum regions (Table 1). The hippocampus also receives major modulatory input from the serotonergic, noradrenergic and dopaminergic transmitter systems as well as from the medial septal nucleus (cholinergic neurons) via the fimbria/fornix pathway.[6] The perforant path has been proposed to be vulnerable in AD pathogenesis due to (i) synaptic loss observed in the OML of AD and mild cognitive impairment cases[7,8]; (ii) the presence of AD-hallmarks, such as amyloid plaques and neurofibrillary tangles, both in the EC[9–11] and in the OML[11,12]; and (iii) substantial loss of EC neurons in AD cases, particularly of layer II,[13–15] as well as loss of cholinergic input to the hippocampus.[16]

In order to further delineate the synaptic pathology of OML in AD brain, we recently performed a proteomic study of microdissected OML from five AD (NFT Braak stage IV and amyloid C) and five control cases.[17] We found that a large number of presynaptic proteins were significantly decreased in the OML of AD brains, whereas postsynaptic proteins were relatively spared. In addition, extensive pathway analysis indicated that synaptic vesicle cycling and exocytosis as prominently affected pathways in the OML of AD brains. The current work is an extension of this earlier publication, where we investigate the specificity and the mechanisms leading to the alteration of presynaptic proteins by performing immunofluorescent stainings in hippocampal sections from human AD and control cases. We selected five synaptic proteins: complexin-1 (CPLX1), synaptotagmin-1 (SYT1), syntaxin-1A (STX1A), synaptogyrin-1 (SYNGR1) and vesicle-associated membrane protein 2 (VAMP2), based on the extent of their reduction determined in our proteomic assay,[17] their presynaptic function and the availability of validated antibodies.

STX1A, SYT1 and VAMP2 are all part of the core synaptic vesicle-membrane-fusion machinery and thus play important roles in neurotransmission.[18] STX1A together with the synaptic vesicle protein VAMP2 and the plasma membrane protein SNAP-25 form the soluble NSF-attachment protein receptor (soluble NSF-attachment protein receptor) complex,[19,20] which is the key component of membrane fusion machinery in exocytosis.[18] SYT1 is a synaptic vesicle protein that acts as a Ca^{2+} sensor[21]; increased levels of Ca^{2+} in the presynaptic terminal triggers an interaction between SYT1 and the plasma membrane protein STX1A that is important for synaptic vesicle exocytosis.[22] Moreover, complexins, such as CPLX1, bind to soluble NSF-attachment protein receptor complexes,[23] participate in Ca^{2+}-triggered exocytosis,[24] and therefore are essential for neurotransmitter release.[25] Among these proteins, the synaptic vesicle protein SYNGR1 is the least studied. Although its exact function still remains unknown, earlier studies suggest that SYNGR1 is most likely not essential for exocytosis,

Table 1 Summary of afferents and efferents of the hippocampus

Afferents			Efferents		
OML	(1)	Perforant path fibres from entorhinal cortex layer II	Granule cell layer	(1)	CA3 via mossy fibres
IML	(1)	Associational/commissural fibres from hilus			
	(2)	CA3 collaterals			
	(3)	Septal fibres			
	(4)	Fibres from thalamus			
CA3-LUC	(1)	Mossy fibres from hilus	CA3	(1)	CA1 via Schaffer collaterals
	(2)	Fibres from locus coeruleus			
CA3-RAD	(1)	CA3 associational fibres			
	(2)	Septal fibres			
CA3-LM	(1)	Perforant path fibres from entorhinal cortex layer II			
	(2)	Septal fibres			
	(3)	Fibres from locus coeruleus			
CA1-RAD	(1)	Schaffer collaterals from CA3	CA1	(1)	Entorhinal cortex layer V via Subiculum
	(2)	Recurrent collaterals from CA1			
	(3)	Fibres from amygdaloid complex			
CA1-LM	(1)	Perforant path fibres from entorhinal cortex layer III			
	(2)	Fibres from thalamus			
	(3)	Fibres from amygdaloid complex			

but it may play a regulatory role in synaptic plasticity, and therefore, neurotransmitter release.[26]

Although decreased mRNA and/or protein levels of these five presynaptic markers have been previously detected in AD brain,[27–30] these studies have so far been performed on homogenates prepared from cortical or hippocampal bulk tissue, thus not allowing any detailed examination of different hippocampal sub-regions. Here, we investigated the distribution of presynaptic proteins in 10 hippocampal sub-regions of control versus advanced AD cases using immunofluorescence. We observed a reduction of presynaptic protein staining densities in the OML consistent with the reduction determined in our proteomic approach. Interestingly, this reduction appeared to be specific to the OML since all others hippocampal sub-regions examined, displayed a similar expression level between controls and AD cases. In order to depict what underlying causes might be responsible for the observed changes in the presynaptic proteins in AD OML, we further investigated both post- and presynaptic compartments by assessing: (i) staining density of postsynaptic protein and a dendritic marker, (ii) the relative number of dentate granule cells, and finally (iii) the staining densities of axonal markers. Finally, we investigated a possible mechanism involving the major AD hallmarks, amyloid plaques and phosphorylated-Tau.

Materials and methods

Ethical approval and consent to participate

The use of human brain material was approved by the ethical and research committees after the consent of patients or relatives for research use. Paraffin-embedded samples were obtained from The Netherlands Brain Bank, Netherlands Institute for Neuroscience, Amsterdam (www.brainbank.nl). All Material has been collected from donors from whom a written informed consent for a brain autopsy and the use of the material and clinical information for research purposes had been obtained by the NBB.

Post-mortem human brain tissues

Formalin-fixed paraffin-embedded hippocampal sections (5 μm thick) from eight sporadic AD and seven non-demented control cases were obtained from the Netherlands Brain Bank. AD cases were clinically diagnosed according to previously published research criteria[31] and pathologically confirmed by the presence of amyloid plaques and neurofibrillary tangles. On the other hand, control cases showed no sign of dementia and presented no or little pathological alterations including a few plaques and tangles. The demographic characteristics of AD and control cases are shown in Table 2. All donors or their next-of-kin gave informed consent. The establishment of the Netherlands Brain Bank was approved the Independent Review Board of VU University Medical Center in Amsterdam, the Netherlands (2009/148).

Immunofluorescence

Hippocampal sections were first deparaffinized in xylene (≥98.5%, AnalaR NORMAPUR® ACS, Reag. Ph. Eur. analytical reagent) and then rehydrated using the following wash steps: 99%, 95% and 70% ethanol, and distilled water. Subsequently, heat-induced antigen retrieval was done using citrate buffer [10 mM citric acid (Sigma Aldrich), with 0.05% Tween-20 (Sigma Aldrich), pH 6] at 110°C for 30 min inside a pressure cooker (Biocare

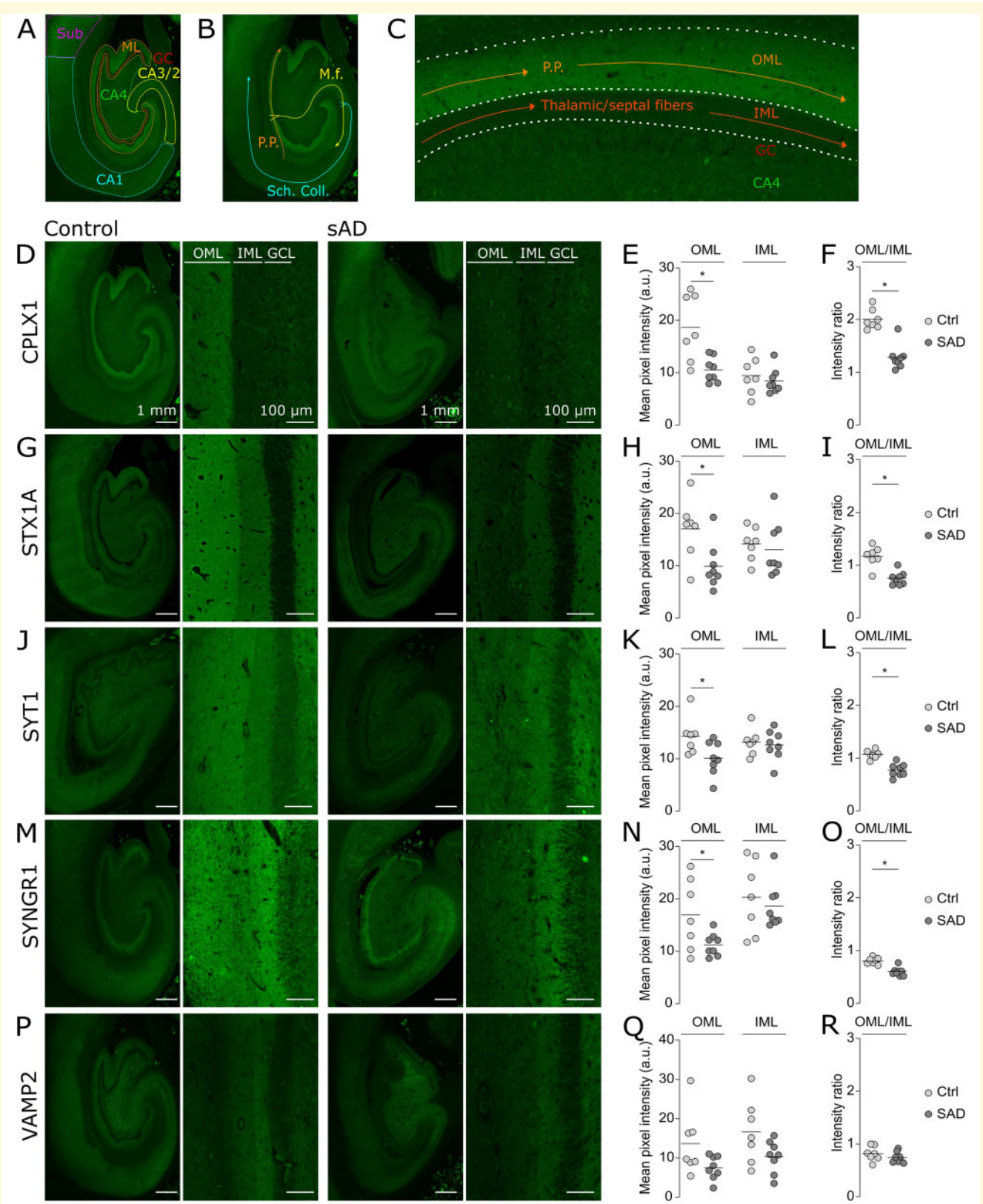

Figure 1 OML-specific reduction in presynaptic proteins. (**A**) Schematic diagram showing the main hippocampal sub-regions in a section labelled for CPLX1 in a healthy hippocampus. (**B**) Schematic diagram showing the hippocampal trisynaptic circuit. (**C**) Schematic diagram showing the main afferents projections in OML and IML. (**D**, **G**, **J**, **M**, **P**) Representative images of the whole hippocampus and zoom-in pictures of the molecular region of the DG in controls (left) and AD (right) brain sections labelled respectively for CPLX1, STX1A, SYT1, SYNGR1, VAMP2. The regions of interests are indicated by outer molecular layer (OML) and inner molecular layer (IML), which are located right next to the granule cell layer (GCL). Scale bar is 1 mm (low magnification) and 100 µm (high magnification). (**E**, **H**, **K**, **N**, **Q**) Scatter plots of the mean pixel

Table 2 Clinical and neuropathological details of cases

Case	Diagnosis	Gender	Age	PMI (h)	Brain pH	APOE status	Braak tau stage	Amyloid stage
1	C	F	73	7.5	NA	44	I	B
2	C	F	84	6	7.65	33	II	B
3	C	F	76	7	6.87	33	II	O
4	C	F	81	5.5	6.77	33	III	A
5	C	F	84	5.5	6.68	33	II	A
6	C	F	83	6	6.6	44	II	B
7	C	F	82	5	6.34	33	II	B
8	AD	F	85	6	6.35	44	V	C
9	AD	F	90	4.5	6.39	33	VI	C
10	AD	F	70	5	6.73	33	V	C
11	AD	F	91	6.5	6.01	44	V	C
12	AD	F	70	6	6	33	VI	C
13	AD	F	80	4	6.26	44	VI	C
14	AD	F	70	4	6.42	44	VI	C
15	AD	F	86	5	6.2	33	VI	C
	P-value	NS	NS	NS	NS	NS	0.0002	0.0002

The clinical and pathological characteristics were compared between AD and control groups using either Student's *t*-test (age, PMI and brain pH) or Mann–Whitney test (ApoE status, Braak), and *P*-value <0.05 considered statistically significant.

Medical). Slides were then washed in PBS with 0.05% Tween-20 (PBS-T) and were subsequently blocked with normal goat serum (Thermo Fisher Scientific) for 20 min at room temperature (RT). Slides were incubated with the primary antibodies listed in Table 3 for 2 h at RT. In order to reduce autofluorescence, slides were then incubated with 1× TrueBlack® Lipofuscin Autofluorescence Quencher (Biotium), which was diluted in 70% ethanol, for 5 min at RT. Subsequently, sections were washed with 1× PBS for three times, which was followed by the incubation with the secondary antibodies (anti-rabbit, anti-mouse and anti-guinea pig IgG conjugated to Alexa 488 or Alexa 568, Thermo Fisher Scientific, 1:500 dilution) for 2 h at RT. Sections were washed with 1× PBS for three times and incubated with either 5 µM of Methoxy X04 (Tocris Bioscience) for 20 min at RT or 300 nM of DAPI for 10 min at RT. Finally, sections were washed in 1× PBS three times and in distilled water, cover-slipped using Fluoromount™ (Southern Biotech) and air-dried overnight at RT. In order to avoid inter-experimental variability, sections from all AD and control cases were stained with a certain antibody at the same time.

Additionally, we assessed the specificity of the fluorescent signal coming from the secondary antibodies by performing several control experiments. In the first experiment, we tested the presence of non-specific fluorescence signal that can be caused by the secondary antibody itself, and incubated consecutive hippocampal sections from a healthy control case with either primary (i.e. STX1A and SYT1) and secondary antibodies (i.e. Alexa 488 and Alexa 568) or only secondary antibodies. In the second experiment, we tested the efficiency of TrueBlack to remove the endogenous autofluorescence coming from the tissue (Jordá-Siquer et al. unpublished results).

Imaging and image analysis

Slides were loaded into the semi-automated Nanozoomer 2.0HT slide scanner (Hamamatsu) and scanned using FITC (green), TRITC (red) and DAPI channels at 20× magnification and fixed additional lens 1.75× (resolution of 454 nm/pixel). Each human case was represented by one hippocampal section. Image acquisitions and settings

intensity of the fluorescent labelling in OML and IML respectively for CPLX1, STX1A, SYT1, SYNGR1, VAMP2. The fluorescence pixel intensities were significantly decreased in AD cases by 44% for CPLX1 (**E**, ctrl: 18.7 ± 6.4, AD: 10.6 ± 2.4; *P*-value = 0.0051), 42% for STX1A (**H**, ctrl: 17.1 ± 5.7, AD: 9.9 ± 4.4; *P*-value = 0.016), 29% for SYT1 (**K**, ctrl: 14.3 ± 3.6, AD: 10.1 ± 3.2; *P*-value = 0.031) and 34% for SYNGR1 (**N**, ctrl: 16.9 ± 6.8, AD: 11.3 ± 2.2; *P*-value = 0.042). In contrast, the levels of these proteins were not altered in the IML of AD cases. (**Q**) The levels of VAMP2 showed a non-significant reduction by 45% (ctrl: 13.7 ± 8.2, AD: 7.5 ± 3.0; *P*-value = 0.068) and 38% (ctrl: 16.6 ± 8.2, AD: 10.3 ± 4.1; *P*-value = 0.075) both in the OML and the IML, respectively. Note that in a healthy brain, CPLX1, STX1A and SYT1 displayed a stronger IR in the OML with respect to IML (**D**, **G**, **J**), while SYNGR1- and VAMP2-IR was more prominent in the IML than the OML (**M**, **P**). (**F**, **I**, **L**, **O**, **R**) Scatter plots of the mean pixel intensity OML/IML ratio of the fluorescent labellings respectively for CPLX1, STX1A, SYT1, SYNGR1, VAMP2. The ratios were significantly decreased in AD cases by 36% for CPLX1 (**F**, ctrl: 2.0 ± 0.2, AD: 1.3 ± 0.2; $P<0.0001$), 35% for STX1A (**I**, ctrl: 1.2 ± 0.2, AD: 0.8 ± 0.1; $P=0.0003$), 28% for SYT1 (**L**, ctrl: 1.1 ± 0.1, AD: 0.8 ± 0.1; $P=0.0001$) and 25% for SYNGR1 (**O**, ctrl: 0.8 ± 0.1, AD: 0.6 ± 0.1; $P<0.0001$). The ratio for VAMP2 was unaltered. Statistical descriptions are described as mean ± S.D. *P*-values refer to unpaired, two-tailed *t*-test.

Table 3 The list of primary antibodies used in this study

Antibodies	Source	Dilution
CPLX1 antibody, rabbit polyclonal	#10246-2-AP, Protein Tech	1:500
STX1A antibody, rabbit polyclonal	#ANR-002, Alomone	1:1000
SYNGR1 antibody, mouse monoclonal	#103011, Synaptic Systems	1:500
SYT1 antibody, mouse monoclonal	#105011, Synaptic Systems	1:500
VAMP2 antibody, mouse monoclonal	#104211, Synaptic Systems	1:500
MBP antibody, rabbit monoclonal	#ab216668, Abcam	1:500
Aβ 1–16 antibody (DE2), mouse monoclonal	#MAB5206, Sigma Aldrich	1:500
Phospho-Tau antibody, mouse monoclonal	#MN1060 Thermo fisher scientific	1:500
SMI-312 antibody, Purified anti-neurofilament marker, mouse polyclonal	#837904, BioLegend	1:500
SHANK2 antibody, guinea pig polyclonal	#162204, Synaptic Systems	1:500
Tau-1 antibody, mouse monoclonal	#MAB3420, Sigma-Aldrich	1:500
MAP2 antibody, mouse monoclonal	#M4403, Sigma-Aldrich	1:500
NeuN antibody, rabbit polyclonal	#ABN78, Merck	1:500

were kept constant for all sections stained with a certain antibody. Additionally, to avoid biases in fluorescence intensity, all AD and control cases were also scanned together. Gamma correction of 1 was applied to all images in order to reach linearity in fluorescence signal and images were then exported as tiff files using the NDP.view2 software (Hamamatsu) and analysed using ImageJ Fiji (NIH).

Semi-quantitative assessment of fluorescence pixel intensity of CPLX1, STX1A, SYT1, SYNGR1 and VAMP2 stainings was carried out in the following sub-regions of the hippocampus: Molecular layers of the dentate gyrus [inner molecular layer (IML) and OML], molecular layers of CA3 (CA3-LUC, CA3-RAD, CA3-LM), molecular layers of CA1 (CA1-RAD and CA1-LM) as well as the neuronal layers like CA4, CA3 and CA1. One image per subfield per case was exported and the mean pixel intensity of each subfield was measured blindly as the average from 5 region of interests. The background was measured from areas outside the tissue for each case and each synaptic marker using the same settings (same magnification and gamma correction of 1). The mean pixel intensity was measured from 2 ROIs and the average was then subtracted from the actual density readings of synaptic markers.

In order to explore changes occurring in the presynaptic and postsynaptic compartments, we did densitometric analysis of three axonal markers (myelin basic protein, SMI-312 and Tau) as well as of a postsynaptic density marker (SH3 and multiple ankyrin repeat domains protein 2) and a dendritic marker [microtubule-associated protein 2 (MAP2)] in the OML and the adjacent IML. Additionally, we measured the neuronal density of the dentate granule cells, which were normalized to the total surface area (mm2), by using neuronal nuclei and DAPI stainings in a blinded fashion. Similarly, amyloid and phosphorylated Tau burden were determined by measuring the mm^2 area in each of the synaptic regions of interest normalized to the total surface of the analysed region.

Statistical analysis

GraphPad Prism 8.0 (GraphPad Software, La Jolla, CA, USA) was used to perform all the statistical analyses. Experimental data were first tested for normal distribution using Kolmogorov-Smirnov tests. The presence of outliers was also checked by the ROUT (default) method. Data were represented using scatter plots in which the mean or median was included or as combined scatter plots with histograms. Normally distributed data were compared by using a two-tailed *t*-test and data that were non-normally distributed were compared using a two-tailed Mann-Whitney rank test. One-way ANOVA was used for analysis of one factor over several groups (analysis of amyloid and P-Tau burden over hippocampal sub-regions) and represented as histograms with error bars (±SEM). Differences between groups were considered statistically significant when $P < 0.05$.

Data availability

The data that support the findings of this study are available from the corresponding author upon reasonable request.

Results

We investigated the specificity and the mechanisms leading to the alteration of presynaptic proteins in AD by comparing hippocampus sections from AD ($n = 8$) and control ($n = 7$) patients from the Netherlands Brain Bank. There were no statistically significant differences in gender, age, postmortem interval, ApoE status, or brain pH between the two groups, while NFT Braak and amyloid stages showed statistically significant differences, as expected (Table 2).

We used an immunofluorescence approach combining an antigen retrieval and autofluorescence quenching methods (see absence of auto-fluorescence in controls; Supplementary Fig. 1A) to label synaptic proteins in

fixed, paraffin-embedded sections of human brain tissue. The sections were imaged with a Nanozoomer 2.0HT slide scanner (Hamamatsu) allowing the acquisition of full sections without mosaicism and a resolution of 454 nm/pixel (55 947 DPI). The thickness of the sections of 5 µm was not suitable to stereological approaches. Taking advantage of the linearity of the fluorescent signal, we measured the immunostaining intensity which is related to the abundance of protein epitopes and thus is indicative of protein abundance. We calculated the mean fluorescent pixel intensities of synaptic proteins in different anatomical regions to evaluate the distribution of synaptic alterations in AD.

Marked reduction of presynaptic proteins levels in the OML in AD

The fluorescence pixel intensities of the five presynaptic proteins CPLX1, STX1A, SYT1, SYNGR1 and VAMP2 were measured in the OML and IML of the dentate gyrus. Interestingly, we found that these proteins displayed different spatial distribution between IML and OML. In a control brain, staining with antibodies directed against CPLX1, STX1A and SYT1 gave rise to a stronger immunoreactivity (IR) in OML than in IML (Fig. 1D, G, J and Supplementary Fig. 1B–D), while SYNGR1 and VAMP2 appeared to be more abundantly expressed in IML than in OML (Fig. 1M, P and Supplementary Fig. 1E and F). The region-specific distribution of these presynaptic proteins created a visible line in the molecular layer, thus allowing us to easily separate IML and OML by gross visualization (Fig. 1).

Semi-quantitative densitometric analysis showed that the staining densities of CPLX1 (44% decrease, *P*-value = 0.0051, Fig. 1D and E), STX1A (42% decrease, *P*-value = 0.016, Fig. 1G and H), SYT1 (29% decrease, *P*-value = 0.031, Fig. 1J and K) and SYNGR1 (34% decrease, *P*-value = 0.042, Fig. 1M and N) were significantly reduced in OML in AD compared to control cases, whereas there was a non-significant decreased tendency in the same direction for VAMP2 staining (45% decrease, *P*-value = 0.068, Fig. 1P and Q). These reductions in staining intensity indicate a decrease in presynaptic protein abundance and do not necessarily reflect a reduction in the number of synapses.

Interestingly, we observed no profound changes between the two groups in the levels of these presynaptic proteins in the IML which receives afferents from the medial septum,[27] the thalamus[10] and the hilus of the dentate gyrus[9] (Fig. 1D–R). Importantly, when the mean pixel intensity of a synaptic protein in OML was normalized to the intensity of the same protein in IML, the ratio was significantly decreased for CPLX1, STX1A, SYT1 and SYNGR1 but not for VAMP2 (Fig. 1F, I, L, O, and R). This analysis ensured that the phenotype observed in OML was not due to a general decrease in staining intensity in AD condition and gave further support to the notion of a specific impairment of OML compared to IML.

Presynaptic protein staining reduction in AD hippocampus specific to the OML

The marked difference in the reduction of presynaptic proteins in OML compared to IML indicates that the synaptic alterations depend on the afferent inputs within a brain sub-region. This led us to investigate whether other hippocampal sub-regions could be affected—which might be innervated by other modalities. The OML receiving abundant afferents from the EC, we hypothesized that other hippocampal sub-regions receiving EC projections (Table 1) could be affected. Thus, in addition to the OML and IML, we analysed the fluorescence pixel intensities of CPLX1, STX1A, SYT1, SYNGR1 and VAMP2 in eight different sub-regions of the hippocampus visible on the same sections, categorized into two groups: (i) molecular layers, enriched in synapses, consisting of CA3-LUC, CA3-RAD, CA3-LM, CA1-RAD and CA1-LM, and (ii) neuronal layers, consisting of CA4, CA3 and CA1 neuronal layers. Despite the observed reduction in CPLX1, SYT1, SYNGR1 levels in AD OML, no significant reductions were detected in any other investigated molecular layers in AD compared to control cases (Fig. 2A–J) or between neuronal layers (see pictures in Fig. 1 and quantifications in Supplementary Fig. 2). Interestingly, the cell-surface soluble NSF-attachment protein receptor protein STX1A exhibited a markedly different staining profile in AD than the vesicular or cytosolic presynaptic proteins described above. Indeed, a marked increase in STX1A staining was observed in the CA4 neuronal layer of AD cases compared to controls (36% increase, *P*-value = 0.048, Supplementary Fig. 2B). Moreover, non-significant trends towards increased levels of STX1A were detected also in the CA3 neuronal layer (52% increase, *P*-value = 0.0506), CA3-LUC (55% increase, *P*-value = 0.08), CA3-RAD (34% increase), CA1 neuronal layer (18% increase), and CA1-RAD (31% increase, *P*-value = 0.09) (molecular layers in Fig. 2B; neuronal layers in Supplementary Fig. 2B).

Preserved postsynaptic compartment in OML of AD cases

The observation of reduced levels of presynaptic proteins in OML raised the question of whether the postsynaptic proteins were also reduced, as expected from the hypothesis of an overall synaptic loss. We assessed the levels of the standard markers of postsynaptic density and dendrites, respectively SH3 and multiple ankyrin repeat domains protein 2 and MAP2. Despite the presence of

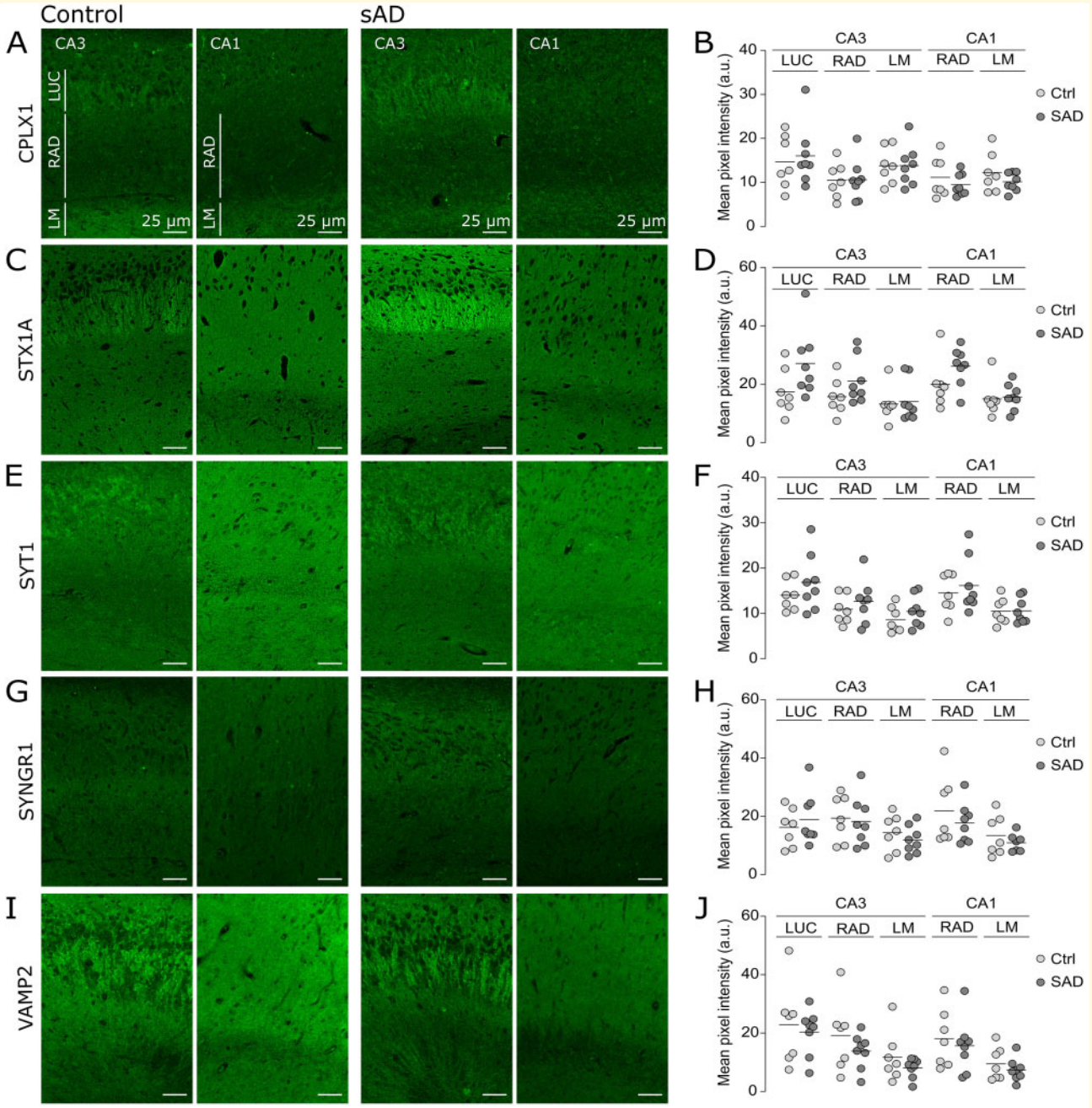

Figure 2 Preserved level of presynaptic proteins in various molecular layers of the hippocampus. (**A**, **C**, **E**, **G**, **I**) Representative images of the CA3 and CA1 regions in controls (left) and AD (right) brain sections labelled respectively for CPLX1, STX1A, SYT1, SYNGR1, VAMP2. The region of interests stratume lucidum (LUC), radiatum (RAD) and lacunosum moleculare (LM) are indicated. (**B**, **D**, **F**, **H**, **J**) Scatter plots of the mean pixel intensity of the fluorescent labelling in OML and IML respectively for CPLX1, STX1A, SYT1, SYNGR1, VAMP2. The mean pixel intensities were not altered between AD and control groups in the molecular layers of the CA3 and CA1. However, non-significant trends towards increased levels of STX1A were detected also in the CA3-LUC (**D**, ctrl: 17.5 ± 7.9, AD: 27.1 ± 11.4; $P = 0.08$) and CA1-RAD (**D**, ctrl: 15.8 ± 6.1, AD: 21.1 ± 7.8; $P = 0.09$). Scale bar is 25 µm.

severe NFT Braak and amyloid stages among the AD cases, the levels of SH3 and multiple ankyrin repeat domains protein 2 and MAP2 were not reduced in AD compared to controls (Fig. 3A–D). Furthermore, we investigated the density of dentate granule cells, the dendrites of which are located at the OML forming synapses with the perforant path termini and noted that there was no obvious reduction in granule cells density in AD compared to control cases (Fig. 3E and F). Together, these results advocate for a distinctive impairment of presynaptic proteins in OML synaptic inputs rather than an overall synaptic loss.

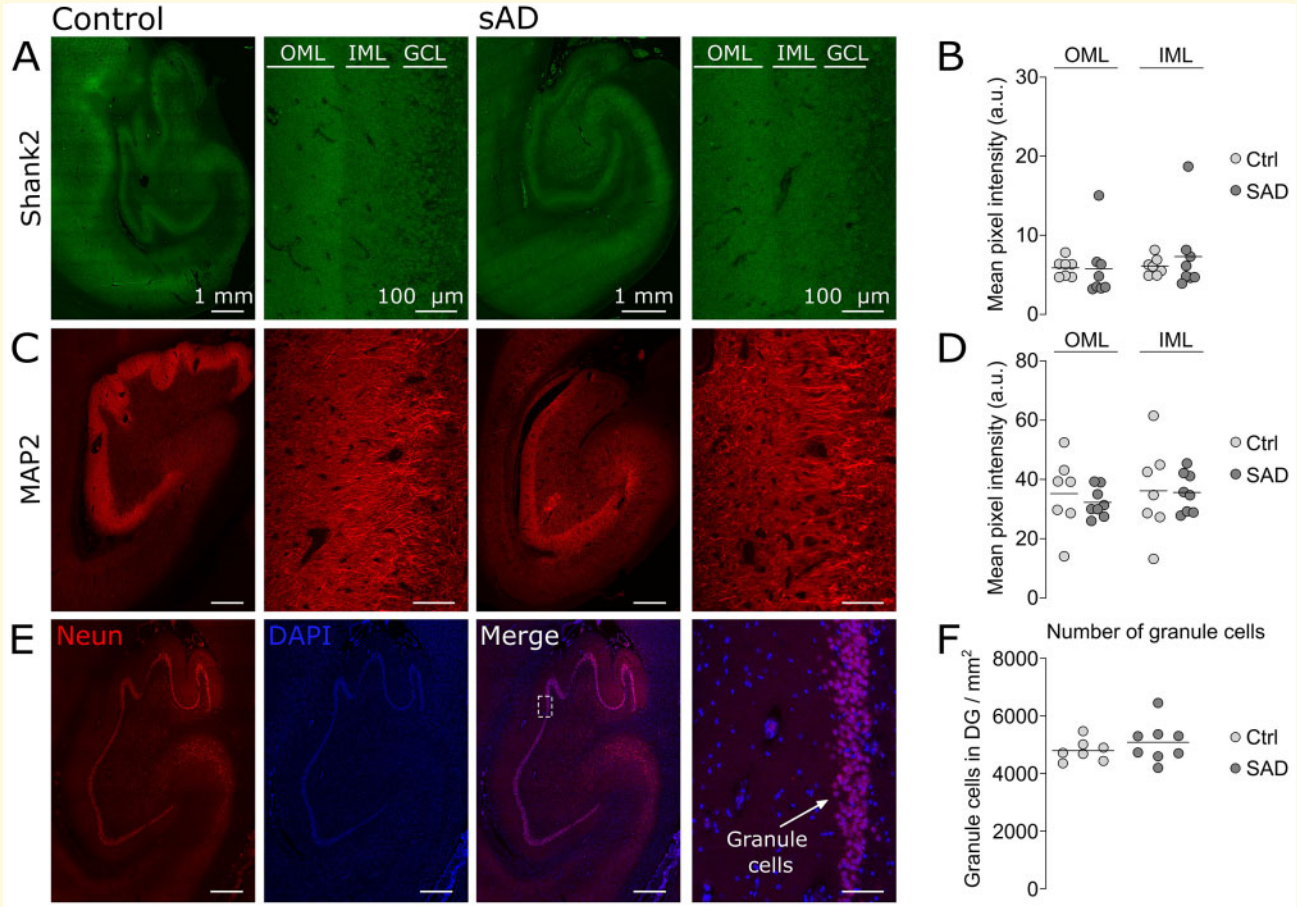

Figure 3 Preserved postsynaptic compartment in AD OML. (**A**, **C**, **E**) Representative images of the whole hippocampus and zoom-in pictures of the molecular region of the DG in controls (left) and AD (right) brain sections labelled respectively for Shank2, MAP2 and colabelled for NeuN and DAPI. The regions of interests are indicated by inner molecular layer (IML) and outer molecular layer (OML), which are located right next to the granule cell layer (GCL). Scale bars are 1 mm (low magnification) and 100 µm (high magnification). (**B**, **D**) Scatter plots of the mean pixel intensity of the fluorescent labellings in OML and IML respectively for Shank2 and MAP2. The levels of SHANK2 and MAP2 were not altered. (**F**) Scatter plots of the mean pixel intensity of the neuronal density (number of dentate granule cells per mm^2) did not show a difference between AD and control groups.

Evidence for maintained axonal projections in AD OML

We next investigated potential mechanisms involved in alterations of presynaptic proteins in OML in AD. One potential mechanism would be if a reduction of axonal projections to the OML would proportionally lead to a reduced amount of presynaptic proteins in this region. Consecutive hippocampal sections from AD and control cases were stained with three different axonal markers: Myelin basic protein (myelin basic protein; for myelinated axons), SMI-312 (for phosphorylated neurofilaments M and H) and the commonly used axonal marker total Tau. Semi-quantitative densitometric assessment showed no difference in the levels of above-mentioned axonal markers between the two groups (Fig. 4A–F) suggesting that biological mechanisms other that a reduction in afferent fibres density are at play in the alterations in presynaptic proteins in OML.

Relationship of presynaptic failure with AD pathology

To further explore the mechanisms behind the specific impairment in presynaptic proteins in OML, we investigated the presence of AD-related pathological hallmarks in the different hippocampal sub-regions of interest. We immuno-labelled amyloid plaques with an antibody against Aβ peptides (clone 6E10) and pathological forms of Tau with an antibody against its phosphorylated isoforms (AT8). Dense core amyloid plaques were distinctly observable in AD cases whereas they were absent from the controls (Fig. 5A). The extent of the amyloid burden

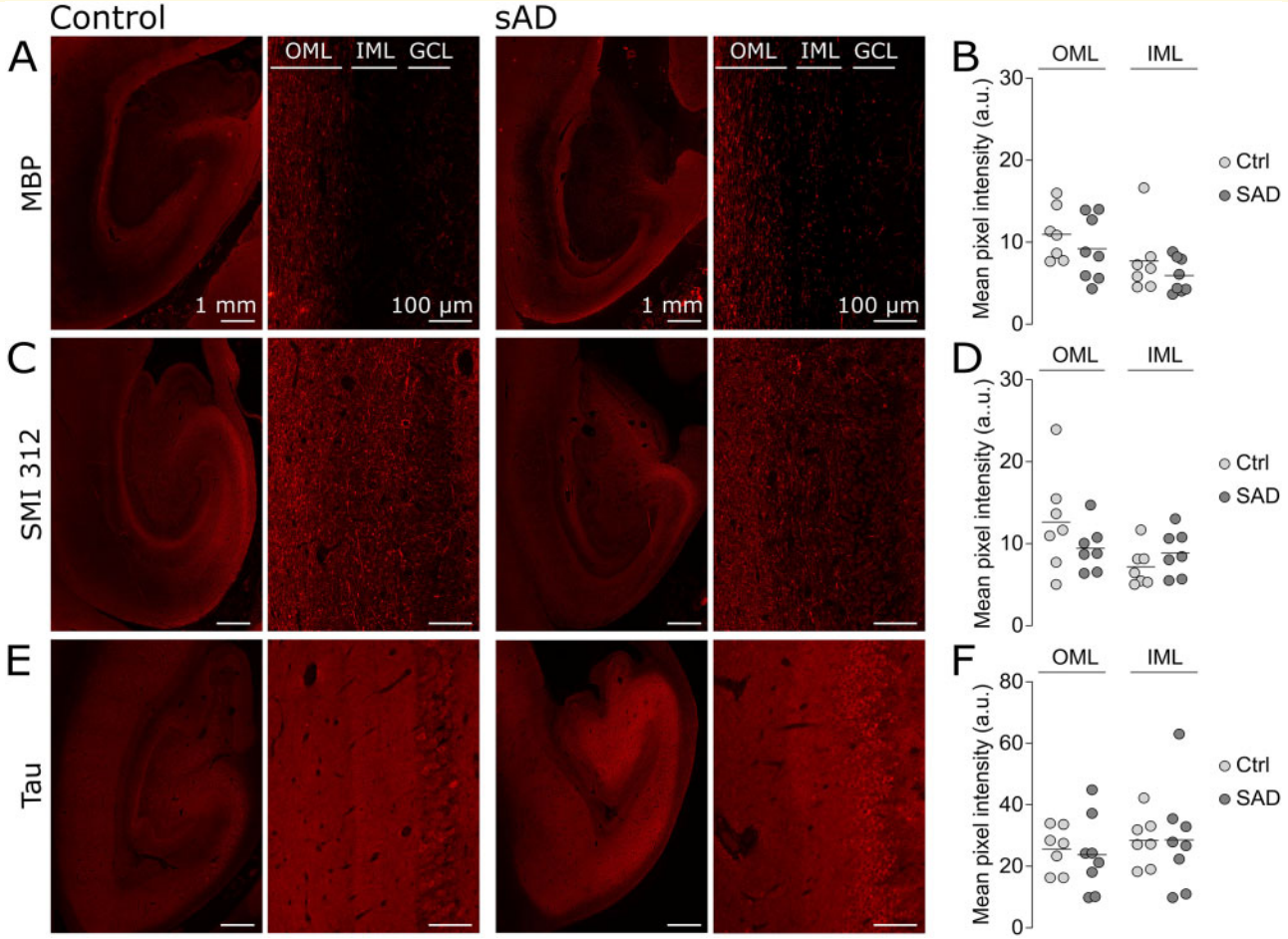

Figure 4 Evidence for maintained axonal projections in AD OML. (**A**, **C**, **E**) Representative images of the whole hippocampus and zoom-in pictures of the molecular region of the DG in controls (left) and AD (right) brain sections labelled respectively for MBP, SMI 312 and Tau. The regions of interests are indicated by outer molecular layer (OML) and inner molecular layer (IML), which are located right next to the granule cell layer (GCL). Scale bars are 1 mm (low magnification) and 100 µm (high magnification). (**B**, **D**, **F**) Scatter plots of the mean pixel intensity of the fluorescent labelling in OML and IML respectively for MBP, SMI 312 and Tau. The levels of MBP, SMI 312 and Tau were not altered.

defined as the total surface covered by Aβ peptides normalized to the surface of the sub-regions analysed was not significantly different between OML and the other hippocampal regions (Fig. 5B). Besides, within OML there was no correlation between amyloid load and the extent of presynaptic proteins reduction among the different AD patients (Fig. 5C). Together, these data indicate that the distinctive reduction in presynaptic proteins in OML cannot be explained by a larger amyloid burden in this sub-region.

The antibody against phosphorylated Tau (AT8) labelled numerous soma in AD cases, in the different CA regions and in the dentate gyrus (Fig. 5D). Strikingly, the abundance of Tau (AT8)-positive neurites was massively higher in AD compared to controls (Fig. 5D). We hypothesized that a higher density of dystrophic neurites, as revealed by phosphorylated Tau (AT8) immunogenicity, could be related to the presynaptic impairment. However, the extent of the burden in dystrophic neurites, i.e. the total surface covered by dystrophic neurites positive for phosphorylated Tau (AT8), normalized to the surface of the sub-region analysed was not significantly different between OML and the other hippocampal molecular layers (Fig. 5E). Finally, within OML there was no correlation between the burden in dystrophic neurites and the extent of presynaptic proteins reduction among the different AD patients (Fig. 5F).

Discussion

Synaptic dysfunction, as revealed by reduction in synaptic proteins[32] as well as loss of synapses,[33] have been observed in early stages of AD. To have a better insight into the molecular mechanisms involved, we previously performed a proteomic analysis of the OML, one of the terminal zones of the perforant path, the main afferent pathway innervating the hippocampus. This approach revealed an impairment of OML

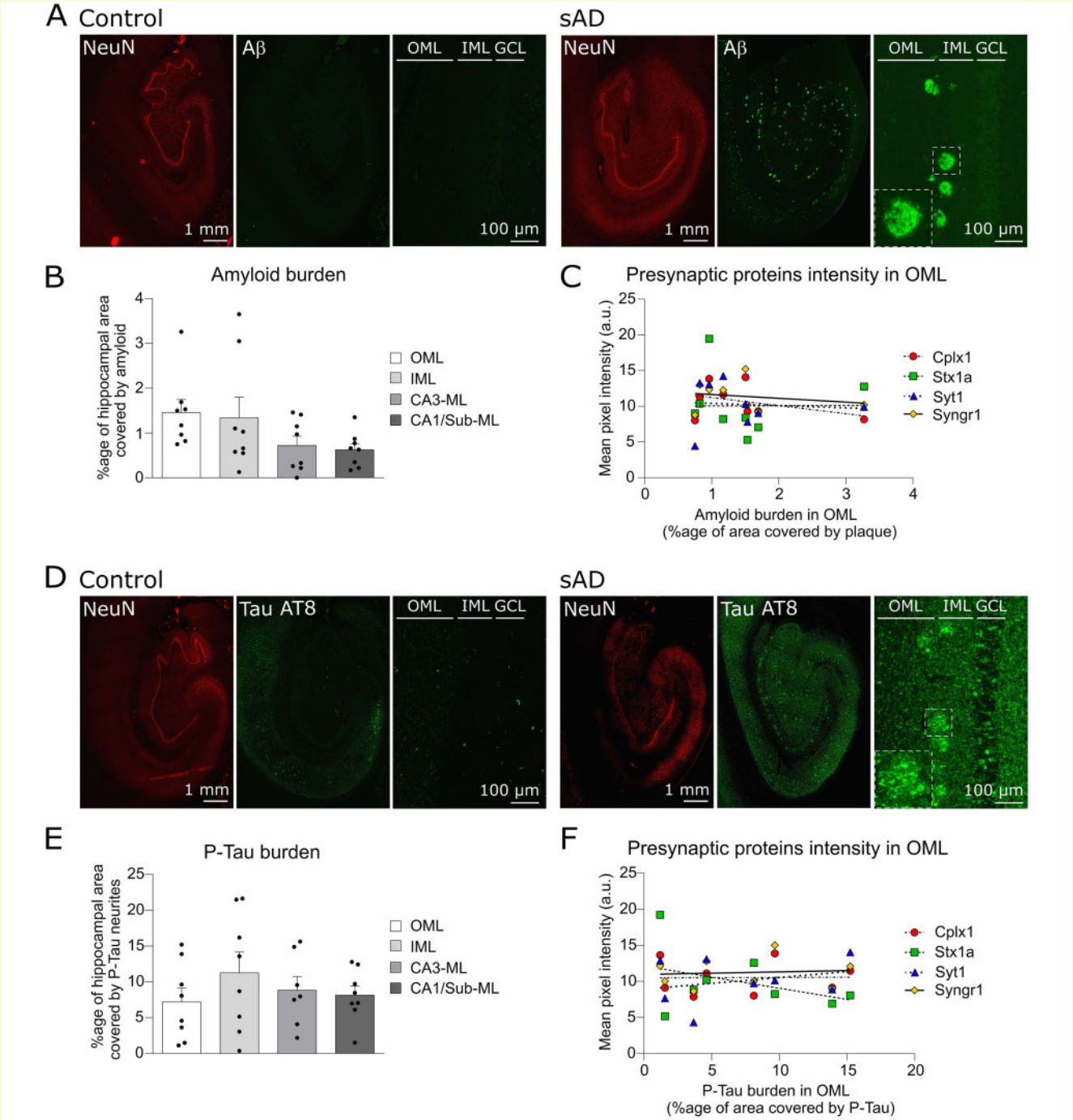

Figure 5 AD-related hallmarks relationship to presynaptic proteins decrease. (**A**) Representative images of the whole hippocampus and zoom-in pictures of the molecular region of the DG in controls (left) and AD (right) brain sections labelled respectively for NeuN and Aβ1-16. The regions of interests are indicated by outer molecular layer (OML) and inner molecular layer (IML) located next to the granule cell layer (GCL). Scale bars are 1 mm (low magnification) and 100 µm (high magnification). (**B**) Scatter plots with bars of the mean percentage of area covered by amyloid staining in different hippocampal molecular layers (OML, IML, CA3-ML, CA1-ML). The amyloid burden is not significantly different between the regions (one-way ANOVA, $P = 0.13$). (**C**) Graph of the mean pixel intensity of the presynaptic protein CPLX1, STX1A, SYT1 and SYNGR1 in OML in function of the amyloid burden. Each dot represents the value of one AD case. There was no correlation between the amyloid burden and the extent of the presynaptic proteins reduction. (**D**) Representative images of the whole hippocampus and zoom-in pictures of the molecular region of the DG in controls (left) and AD (right) brain sections labelled respectively for NeuN and phosphorylated-Tau (AT8). The regions of interests are indicated by outer (OML) and inner (IML) molecular layers located next to the granule cell layer (GCL). Scale bars are 1 mm (low magnification) and 100 µm (high magnification). (**E**) Scatter plots with bars of the mean percentage of area covered by neurites positive for phosphorylated-Tau (AT8) in different hippocampal subregions (OML, IML, CA3, CA1). The dystrophic neurites burden is not significantly different between the regions (one-way ANOVA, $P = 0.56$). (**F**) Graph of the mean pixel intensity of the presynaptic protein CPLX1, STX1A, SYT1 and SYNGR1 in OML in function of the burden in AT8-positive dystrophic neurites. Each dot represents the value in one AD case. There was no correlation between the burden in AT8-positive dystrophic neurites and the extent of the presynaptic proteins reduction.

proteome in AD characterized by a reduced level of presynaptic proteins, whereas the level of the postsynaptic proteins were unchanged.[17] Here, we aimed to expand that study and further explore the distribution of presynaptic proteins across the entire human hippocampus and to investigate the possible causes of the proteomic impairment in OML. We selected five presynaptic proteins, CPLX1, STX1A, SYT1, SYNGR1 and VAMP2, which play important roles in neurotransmission. We performed immunofluorescent staining to assess their expression level assessed across 10 different sub-regions of the hippocampus, categorized into molecular and neuronal layers.

Heterogeneous distribution of key presynaptic proteins in healthy controls

All selected antibodies showed a strong IR in the neuropil but not in the cell soma such as the densely packed dentate granule cell layer, confirming the enrichment of these proteins in synapses. Interestingly, the five proteins displayed a region-specific distribution which allowed a clear visualization of the OML/IML border: CPLX1, STX1A and SYT1 displayed a stronger IR in the OML whereas SYNGR1- and VAMP2-IR appeared to be more abundant in the IML (Fig. 1 and Supplementary Fig. 1B–F). Ramos-Miguel et al. have also detected higher levels of CPLX1 in the OML than in the IML.[34] Albeit both IML and OML contains mainly excitatory inputs to GC, the afferent input is, to a large extent distinct and arises from mossy cells of the CA4 (called associational/commissural projections) and EC layer II, respectively. Thus, it is plausible that the distinctive spatial distribution of the presynaptic proteins occurs as a result of different synapses exhibiting different molecular compositions.[35]

OML-specific presynaptic failure within the hippocampus

The labelling intensity of CPLX1, STX1A, SYT1 and SYNGR1 was significantly reduced in the OML of AD compared to control cases (Fig. 1), corroborating our previous proteomics findings.[17] Interestingly, these reductions were specific to the OML region since all nine other molecular and neuronal sub-regions we examined were preserved, at least in the AD cases examined herein (Fig. 2). Nevertheless, we cannot rule out that subtle reductions were missed due to lack of statistical power. Previous studies based on immunohistochemistry reported a decrease in synapsin and synaptophysin in OML, however, detailed analyses of the distribution of these presynaptic proteins between hippocampal sub-regions were missing.[36,37] In agreement with our study, a decreased ratio of OML/IML levels of synaptic proteins has previously been reported in AD brain, although the potential changes in staining intensity changes in the IML itself was not clearly stated.[38,39] This specificity is intriguing when considering that our cohort consists of AD cases with late stages of AD pathology (NFT Braak stages V-VI and amyloid C; Table 2) and that perforant path afferent input from the EC does not solely project to the OML but also to CA fields. Thus, more than a global failure of the perforant path, our results highlight the specific vulnerability of the pathway projecting to the OML in AD, with specific biological mechanisms for this selective vulnerability not yet revealed.

Possible homeostatic compensation in AD hippocampus

While no profound alterations were detected in the levels of CPLX1, SYT1, SYNGR1 and VAMP2 in any of the other studied hippocampal sub-regions of AD patients, the plasma membrane protein STX1A showed increased immunostaining in the CA4 (Fig. 2). A possible explanation for this finding could be that STX1A levels undergo a compensatory increase in these regions (possibly via increased collateral branching or sprouting) in order to compensate for the reduced input that dentate granule cells receive from the EC layer II, which is evident by the reduced STX1A level in the OML. As opposed to our findings, in a few proteomics study, decreased levels of STX1A were reported in AD brains.[28,29,40] However, these studies have used homogenates prepared from bulk tissue of AD brains, and would not be able to tease out cell- and layer-specific discrete changes as the ones observed in sub-hippocampal regions in the current study. The increase in STXA1 staining in the AD cases is clearly visible (Fig. 2C) but only extends through one layer, and therefore would be hard to discern using whole tissue homogenates.

Specific alteration of OML neurotransmitter release proteins in AD

We next investigated whether the postsynaptic compartment was also altered as expected in the hypothesis of full synapses collapse. When the components of the postsynaptic compartment were investigated, we did not find any alterations in the levels of the postsynaptic density protein SH3 and multiple ankyrin repeat domains protein 2 and the dendritic marker MAP2 in AD (Fig. 3), which were in line with our previous proteomic findings.[17] Furthermore, the density of dentate granule cells, using neuronal nuclei staining, showed no loss of neuronal nuclei staining in AD compared to controls. Taken together, our findings suggest that postsynaptic compartments in the OML are rather intact and the deficit is specifically presynaptic.

However, quantification of postsynaptic densities using structural methods such as electron microscopy indicated that they decrease in AD condition.[8,41,42] Differences between the amount of synaptic protein amounts (as assessed in the present study) and the number of structurally defined synaptic compartments (as assessed by EM) could account for the divergence in results. Indeed, structural analyses have reported that synapse loss is associated with an increase in the length of synaptic appositions (indicating larger synapses),[8] possibly as a compensation by a synaptic homeostasis mechanism. Therefore, the total amount of synaptic proteins may not change in most synaptic fields. This is however not the case of the OML of the DG, where the decrease in the IR of presynaptic proteins, together with the reduction assessed by our previous proteomic approach,[17] advocates for a marked reduction specific to presynaptic proteins. This gives support to the notion of a preferential presynaptic failure in OML of AD brain.[43]

Among the proteins we investigated, CPLX1 was the one with the lowest AD/Control ratio both in the present study and in our previous proteomic study[17] performed on different human cohorts, emphasizing the importance of this protein in AD pathogenesis. In agreement with this, previous reports showed that higher levels of specific presynaptic proteins, including CPLX1, were associated with better cognitive function.[44,45] Before, or in addition to the neurodegeneration occurring in AD, specific alterations in the metabolism of proteins involved in presynaptic plasticity may well contribute to the cognitive impairment.

Neurodegeneration versus retrograde degeneration

The question of the order of the different pathological events occurring during AD progression is important and has not yet been fully answered. For example, to know whether the presynaptic failure occurs before or as a consequence of neurodegeneration is crucial because it will impact the design of future therapeutic approaches. Compelling neuropathological evidence has shown a dramatic and early loss of EC neurons in AD, particularly in layer II, which correlates with cognitive impairment in AD.[13,14] Hence, one theory proposes that the degeneration of EC neurons leads to the loss of perforant path afferents and therefore to synaptic loss and reduced synaptic protein-IR in the terminal zone of the perforant path. Supporting this notion, it has been demonstrated that following an EC lesion, synaptophysin-IR was reduced in the OML in rat brain.[46] One limitation of our study is the absence of quantification of EC neurons in layer II which prevented us to investigate whether the reduction in presynaptic proteins in OML correlated with a loss of neurons projecting perforant path afferents. Indeed, in the brain sections we analysed, the neurons in the para-hippocampal cortex were not distributed in islands as expected for EC layer II, probably due to the posterior position of the sections.

We could nevertheless test if the presynaptic changes at the OML were related to axonal degeneration whether this depends or not on somatic degeneration. We assessed possible structural alteration of the axonal projections in OML by investigating the levels of the myelin basic protein (for myelinated axons), SMI-312 (for phosphorylated neurofilaments M and H) and the commonly used axonal marker Tau. Despite the advanced stage of the AD cases, we did not find significant alterations in the levels of these three markers in the OML (Fig. 4). This observation is apparently inconsistent with a massive degeneration of EC neurons from layer, a scenario in which the number of projecting afferents should be reduced proportionally to the neuronal loss. One possible explanation is that the afferent input from EC only represent a minority of axons passing through the OML or that axonal projections coming from non-degenerated areas compensate for the loss of axons within the perforant path.

An alternative hypothesis is that axonal projections from EC layer II are not massively degenerated. This possibility offers a straightforward explanation for the unchanged labelling intensities of the axonal markers between AD and controls. It also clarifies why all presynaptic proteins are not altered at the same extent between AD and controls.[17] Indeed, if the reduction in presynaptic proteins was directly resulting from a loss of afferent inputs to the OML, similar AD/Control ratio between the presynaptic proteins detected would have been expected. As previously discussed by Terry et al.,[3,47] the loss of neocortical synapses correlates with cognitive decline much better than cell counts and this synaptic loss occurs earlier than death of the neuronal soma. This observation is the basis for the hypothesis of retrograde degeneration which states that synaptic dysfunction precedes axonal degeneration and neuronal death. This hypothesis is supported by a recent observation that changes in synaptic proteins precede neurodegeneration markers in prodromal AD.[48] The data that we collected here are consistent with a retrograde degeneration in which presynaptic proteins are reduced but the axons are not yet degenerated and which, within the hippocampus, would specifically start in the OML.

A retrograde degenerative mechanism could also explain the intriguing observation that the genetic deletion, or the loss of function (using neurotoxins), of several presynaptic proteins leads to neurodegeneration. For example, loss of Munc18 that prevents neurotransmitter release leads to a rapid neurodegeneration.[49–51] In a similar way, genetic deletion of CSPα revealed that it cooperates with α-synuclein and SNAP-25 to prevent neurodegeneration[52–54] and use of botulinum neurotoxins revealed a direct role of STX1A and SNAP-25 in neuron survival.[55,56] Thus, there is a possibility that massive reduction in presynaptic proteins, as seen in the perforant path projecting to the OML, leads to the loss of the

projecting neurons in the EC. The resolution of the cause-consequence relationship between presynaptic failure and somatic degeneration will be one of the next challenges for research on AD. Using populations at different stages in the progression of the pathology, the application to the human brain of clarifying techniques combined to light sheet microscopy[57] will offer new opportunities to investigate the relationship between neurodegeneration in the EC and remote presynaptic alterations in the perforant path axons in the DG-OML.

Homogeneous burden in amyloid plaques and dystrophic neurites across the hippocampus

We searched for a possible pathological correlate of the presynaptic alteration in OML by investigating the extent of the AD-hallmarks in this region compared to the other hippocampal sub-regions. We labelled amyloid plaques with an antibody against Aβ1-16 and observed neuritic and diffuse plaques in all hippocampal regions in AD whereas amyloid plaques were absent in controls (Fig. 5). Notably, the area covered by amyloid plaques was not larger in the OML compared to other molecular layers of the hippocampus (Fig. 5B). In OML, the presynaptic alterations were not proportional to the amyloid burden (Fig. 5C).

In an effort to specially search for a cause of an axonal or presynaptic impairment we focused our attention on the presence of neurites immuno-reactive for phosphorylated-Tau. Indeed, a role of pathological form of tau in the impairment of presynaptic proteins has been recently exemplified by the observation that pathological Tau binds to synaptic vesicles[58,59] leading to a smaller pool of active vesicles and to decreased synaptic transmission.[59] We observed that neurites expressing phosphorylated-Tau were remarkably more abundant in AD compared to controls (Fig. 5D). Interestingly, neurites expressing phosphorylated-Tau were arranged sometimes in islands, for example in the IML (Fig. 5D) likely corresponding to dystrophic neurites around senile plaques.[60] The area covered by neurites expressing phosphorylated-Tau was not larger in OML compared to other molecular layers of the hippocampus (Fig. 5E). Moreover, in OML, the presynaptic alterations were not proportional to the burden in phosphorylated-Tau (Fig. 5F). Thus, with the limitations inherent to our study (i.e. incompatibility with stereological investigations) in mind, our data suggest a lack of correlation between the presynaptic alterations observed in OML and the two AD-related hallmarks we investigated.

In summary, our investigation distinctly highlights the projections to the OML, i.e. the perforant path from EC layer II to dentate granule cells, as a specific vulnerable pathway in AD. Our findings also emphasize that postsynaptic compartments in the OML are rather intact, giving support to the notion of specific presynaptic failure in AD. These findings might lead to novel and more targeted therapy options for the early stages of AD.

Supplementary material

Supplementary material is available at *Brain Communications* online.

Acknowledgements

The postmortem human brain tissue for this study was supplied by the Netherlands Brain Bank (Amsterdam, the Netherlands). We thank all the donors for the tissue used in this study. Imaging was performed at the Bordeaux Imaging Center, a service unit of the CNRS-INSERM and Bordeaux University, member of the national infrastructure France BioImaging (ANR-10-INBS-04).

Funding

This project has received funding from the European Union's Horizon 2020 research and innovation program under the Marie Skłodowska-Curie grant agreement No 676144 (Synaptic Dysfunction in Alzheimer Disease, SyDAD). The project was supported by the grants from Swedish Research Council (VR 2018–02843), Margaretha af Ugglas Stiftelse, Alzheimerfonden, Demensfonden, Stohnes Stiftelse, Stiftelsen för Gamla Tjänarinnor and Fondation Recherche sur Alzheimer. This project was also supported by the Centre National de la Recherche Scientifique, from the foundation Plan Alzheimer, from France Alzheimer, and from the Fondation pour la Recherche Médicale (project #DEQ20160334900). A.C.G. was supported by a grant from the National Institutes on Aging (RF1AG061566). The authors declare that they have no conflicts of interest with the contents of this article.

Competing interests

The authors declare that they have no competing interests.

References

1. DeKosky ST, Scheff SW. Synapse loss in frontal cortex biopsies in Alzheimer's disease: Correlation with cognitive severity. Ann Neurol. 1990;27:457–464.
2. Masliah E, Mallory M, Alford M, et al. Altered expression of synaptic proteins occurs early during progression of Alzheimer's disease. Neurology. 2001;56:127–129.
3. Terry RD, Masliah E, Salmon DP, et al. Physical basis of cognitive alterations in Alzheimer's disease: Synapse loss is the major correlate of cognitive impairment. Ann Neurol. 1991;30:572–580.

4. Ohm TG. The dentate gyrus in Alzheimer's disease. In: HE, Scharfman ed. Progress in brain research. Amsterdam: Elsevier; 2007:723–740.
5. Cappaert NLM, Van Strien NM, Witter MP. Chapter 20—hippocampal formation. In: G, Paxinos ed.The rat nervous system, 4th ed. San Diego: Academic Press; 2015:511–573.
6. Solari N, Hangya B. Cholinergic modulation of spatial learning, memory and navigation. Eur J Neurosci. 2018;48:2199–2230.
7. Scheff SW, Price DA, Schmitt FA, Mufson EJ. Hippocampal synaptic loss in early Alzheimer's disease and mild cognitive impairment. Neurobiol Aging. 2006;27:1372–1384.
8. Scheff SW, Sparks DL, Price DA. Quantitative assessment of synaptic density in the outer molecular layer of the hippocampal dentate gyrus in Alzheimer's disease. Dementia. 1996;7:226–232.
9. Arnold SE, Hyman BT, Flory J, Damasio AR, Van Hoesen GW The topographical and neuroanatomical distribution of neurofibrillary tangles and neuritic plaques in the cerebral cortex of patients with Alzheimer's disease. Cereb Cortex. 1991;1:103-116.
10. Braak H, Braak E. The human entorhinal cortex: Normal morphology and lamina-specific pathology in various diseases. Neurosci Res. 1992;15:6–31.
11. Thal DR, Holzer M, Rüb U, et al. Alzheimer-related tau-pathology in the perforant path target zone and in the hippocampal stratum oriens and radiatum correlates with onset and degree of dementia. Exp Neurol. 2000;163:98–110.
12. Hyman BT, Van Hoesen GW, Kromer LJ, Damasio AR. Perforant pathway changes and the memory impairment of Alzheimer's disease. Ann Neurol. 1986;20:472–481.
13. Gómez-Isla T, Price JL, McKeel DW, Morris JC, Growdon JH, Hyman BT. Profound loss of layer II entorhinal cortex neurons occurs in very mild Alzheimer's disease. J Neurosci. 1996;16: 4491–4500.
14. Kordower JH, Chu Y, Stebbins GT, et al. Loss and atrophy of layer II entorhinal cortex neurons in elderly people with mild cognitive impairment. Ann Neurol. 2001;49:202–213.
15. Price JL, Ko AI, Wade MJ, Tsou SK, McKeel DW, Morris JC. Neuron number in the entorhinal cortex and CA1 in preclinical Alzheimer disease. Arch Neurol. 2001;58:1395–1402.
16. Haam J, Yakel JL. Cholinergic modulation of the hippocampal region and memory function. J Neurochem. 2017;142:111–121.
17. Haytural H, Mermelekas G, Emre C, et al. The proteome of the dentate terminal zone of the perforant path indicates presynaptic impairment in Alzheimer disease. Mol Cell Proteomics. 2020;19: 128–141.
18. Sudhof TC, Rizo J. Synaptic vesicle exocytosis. Cold Spring Harb Perspect Biol. 2011;3:a005637.
19. Sollner T, Whiteheart SW, Brunner M, et al. SNAP receptors implicated in vesicle targeting and fusion. Nature. 1993;362: 318–324.
20. Sutton RB, Fasshauer D, Jahn R, Brunger AT. Crystal structure of a SNARE complex involved in synaptic exocytosis at 2.4 Å resolution. Nature. 1998;395:347–353.
21. Geppert M, Goda Y, Hammer RE, et al. Synaptotagmin I: A major Ca2+ sensor for transmitter release at a central synapse. Cell. 1994;79:717–727.
22. Shao X, Li C, Fernandez I, Zhang X, Südhof TC, Rizo J. Synaptotagmin-syntaxin interaction: The C2 domain as a Ca2+-dependent electrostatic switch. Neuron. 1997;18:133–142.
23. McMahon HT, Missler M, Li C, Sudhof TC. Complexins: Cytosolic proteins that regulate SNAP receptor function. Cell. 1995;83:111–119.
24. Reim K, Mansour M, Varoqueaux F, et al. Complexins regulate a late step in Ca2+-dependent neurotransmitter release. Cell. 2001; 104:71–81.
25. López-Murcia FJ, Reim K, Jahn O, Taschenberger H, Brose N. Acute complexin knockout abates spontaneous and evoked transmitter release. Cell Rep. 2019;26:2521–2530.e5.
26. Janz R, Sudhof TC, Hammer RE, Unni V, Siegelbaum SA, Bolshakov VY. Essential roles in synaptic plasticity for synaptogyrin I and synaptophysin I. Neuron. 1999;24:687–700.
27. Beeri MS, Haroutunian V, Schmeidler J, et al. Synaptic protein deficits are associated with dementia irrespective of extreme old age. Neurobiol Aging. 2012;33:1125.e1-8.
28. Brinkmalm A, Brinkmalm G, Honer WG, et al. Targeting synaptic pathology with a novel affinity mass spectrometry approach. Mol Cell Proteomics. 2014;13:2584–2592.
29. Musunuri S, Wetterhall M, Ingelsson M, et al. Quantification of the brain proteome in Alzheimer's disease using multiplexed mass spectrometry. J Proteome Res. 2014;13:2056–2068.
30. Sze CI, Bi H, Kleinschmidt-DeMasters BK, Filley CM, Martin LJ. Selective regional loss of exocytotic presynaptic vesicle proteins in Alzheimer's disease brains. J Neurol Sci. 2000;175:81–90.
31. Dubois B, Feldman HH, Jacova C, et al. Research criteria for the diagnosis of Alzheimer's disease: Revising the NINCDS-ADRDA criteria. Lancet Neurol. 2007;6:734–746.
32. de Wilde MC, Overk CR, Sijben JW, Masliah E. Meta-analysis of synaptic pathology in Alzheimer's disease reveals selective molecular vesicular machinery vulnerability. Alzheimers Dement. 2016; 12:633–644.
33. Scheff SW, Price DA. Synaptic pathology in Alzheimer's disease: A review of ultrastructural studies. Neurobiol Aging. 2003;24: 1029–1046.
34. Ramos-Miguel A, Sawada K, Jones AA, et al. Presynaptic proteins complexin-I and complexin-II differentially influence cognitive function in early and late stages of Alzheimer's disease. Acta Neuropathol. 2017;133:395–407.
35. O'Rourke NA, Weiler NC, Micheva KD, Smith SJ. Deep molecular diversity of mammalian synapses: Why it matters and how to measure it. Nat Rev Neurosci. 2012;13:365–379.
36. Honer WG, Dickson DW, Gleeson J, Davies P. Regional synaptic pathology in Alzheimer's disease. Neurobiol Aging. 1992;13: 375–382.
37. Lippa CF, Hamos JE, Pulaski-Salo D, Degennaro LJ, Drachman DA. Alzheimer's disease and aging: Effects on perforant pathway perikarya and synapses. Neurobiol Aging. 1992;13:405–411.
38. Masliah E, Mallory M, Hansen L, DeTeresa R, Alford M, Terry R. Synaptic and neuritic alterations during the progression of Alzheimer's disease. Neurosci Lett. 1994;174:67–72.
39. Robinson JL, Molina-Porcel L, Corrada MM, et al. Perforant path synaptic loss correlates with cognitive impairment and Alzheimer's disease in the oldest-old. Brain. 2014;137:2578–2587.
40. Zhang Q, Ma C, Gearing M, Wang PG, Chin L-S, Li L. Integrated proteomics and network analysis identifies protein hubs and network alterations in Alzheimer's disease. Acta Neuropathol Commun. 2018;6:19.
41. Scheff SW, Price DA. Synaptic density in the inner molecular layer of the hippocampal dentate gyrus in Alzheimer disease. J Neuropathol Exp Neurol. 1998;57:1146–1153.
42. Scheff SW, Price DA, Schmitt FA, DeKosky ST, Mufson EJ. Synaptic alterations in CA1 in mild Alzheimer disease and mild cognitive impairment. Neurology. 2007;68:1501–1508.
43. Barthet G, Mulle C Presynaptic failure in Alzheimer's disease. Prog Neurobiol. 2020;194:101801.
44. Honer WG, Barr AM, Sawada K, et al. Cognitive reserve, presynaptic proteins and dementia in the elderly. Transl Psychiatry. 2012;2:E114.
45. Yu L, Tasaki S, Schneider JA, et al. Cortical proteins associated with cognitive resilience in community-dwelling older persons. JAMA Psychiatry. 2020;77:1–9.
46. Cabalka LM, Hyman BT, Goodlett CR, Ritchie TC, Van Hoesen GW. Alteration in the pattern of nerve terminal protein immunoreactivity in the perforant pathway in Alzheimer's disease and in rats after entorhinal lesions. Neurobiol Aging. 1992;13:283–291.
47. Terry RD. Cell death or synaptic loss in Alzheimer disease. J Neuropathol Exp Neurol. 2000;59:1118–1119.

48. Lleó A, Núñez-Llaves R, Alcolea D, et al. Changes in synaptic proteins precede neurodegeneration markers in preclinical Alzheimer's disease cerebrospinal fluid. Mol Cell Proteomics. 2019;18:546–560.
49. Dudok JJ, Groffen AJA, Toonen RFT, Verhage M. Deletion of Munc18-1 in 5-HT neurons results in rapid degeneration of the 5-HT system and early postnatal lethality. PLoS One. 2011;6:E28137.
50. Heeroma JH, Roelandse M, Wierda K, et al. Trophic support delays but does not prevent cell-intrinsic degeneration of neurons deficient for munc18-1. Eur J Neurosci. 2004;20:623–634.
51. Verhage M, Maia AS, Plomp JJ, et al. Synaptic assembly of the brain in the absence of neurotransmitter secretion. Science. 2000; 287:864–869.
52. Chandra S, Gallardo G, Fernández-Chacón R, Schlüter OM, Südhof TC. Alpha-synuclein cooperates with CSPalpha in preventing neurodegeneration. Cell. 2005;123:383–396.
53. Fernández-Chacón R, Wölfel M, Nishimune H, et al. The synaptic vesicle protein CSP alpha prevents presynaptic degeneration. Neuron. 2004;42:237–251.
54. Sharma M, Burré J, Bronk P, Zhang Y, Xu W, Südhof TC. CSPα knockout causes neurodegeneration by impairing SNAP-25 function. EMBO J. 2012;31:829–841.
55. Berliocchi L, Fava E, Leist M, et al. Botulinum neurotoxin C initiates two different programs for neurite degeneration and neuronal apoptosis. J Cell Biol. 2005;168:607–618.
56. Peng L, Liu H, Ruan H, et al. Cytotoxicity of botulinum neurotoxins reveals a direct role of syntaxin 1 and SNAP-25 in neuron survival. Nat Commun. 2013;4:1472.
57. Morawski M, Kirilina E, Scherf N, et al. Developing 3D microscopy with CLARITY on human brain tissue: Towards a tool for informing and validating MRI-based histology. NeuroImage. 2018;182:417–428.
58. Liu C, Song X, Nisbet R, Götz J. Co-immunoprecipitation with Tau isoform-specific antibodies reveals distinct protein interactions and highlights a putative role for 2N Tau in disease. J Biol Chem. 2016;291:8173–8188.
59. Zhou L, McInnes J, Wierda K, et al. Tau association with synaptic vesicles causes presynaptic dysfunction. Nat Commun. 2017;8: 15295.
60. Arai H, Lee VM, Otvos L, et al. Defined neurofilament, tau, and beta-amyloid precursor protein epitopes distinguish Alzheimer from non-Alzheimer senile plaques. Proc Natl Acad Sci USA. 1990;87:2249–2253.